iScience

CellPress
OPEN ACCESS

Article

Cdh1-APC Regulates Protein Synthesis and Stress Granules in Neurons through an FMRP-Dependent Mechanism

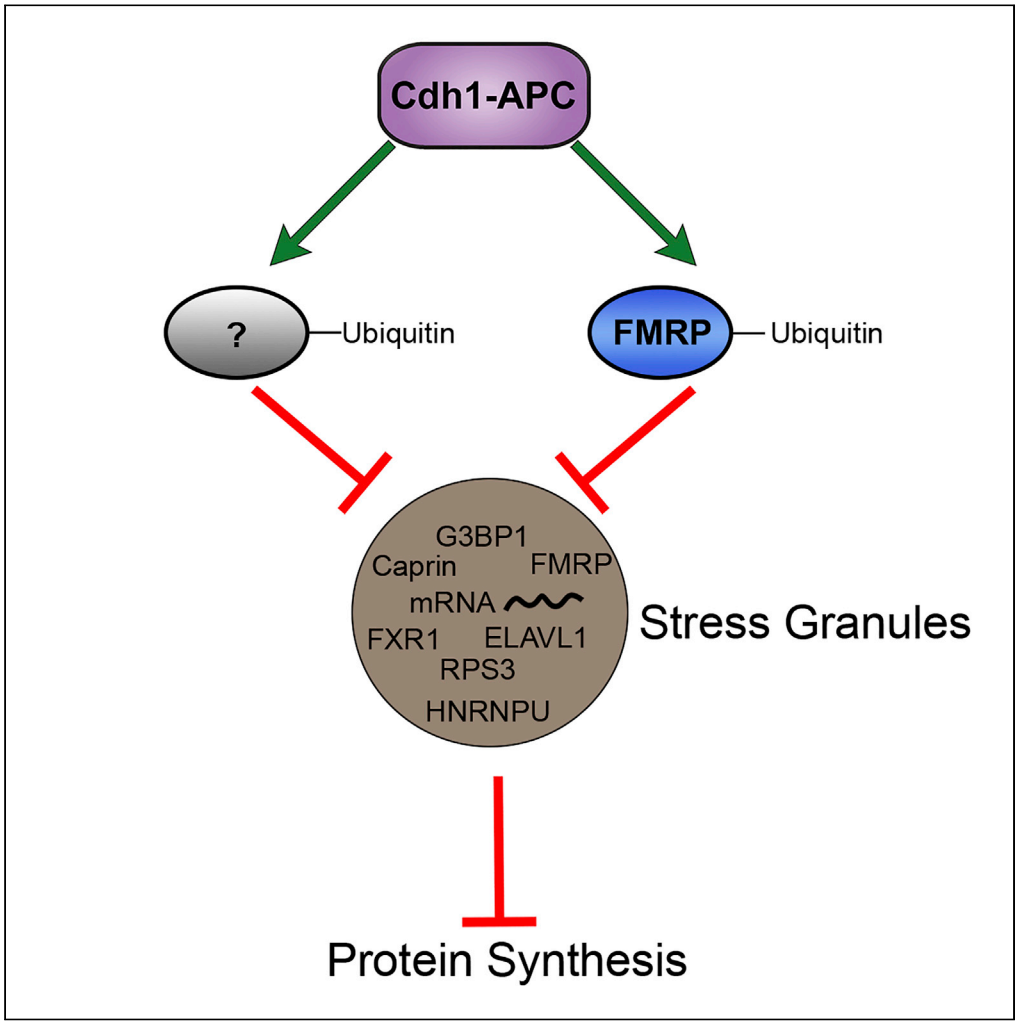

Arielle N. Valdez-Sinon, Austin Lai, Liang Shi, Carly L. Lancaster, Avanti Gokhale, Victor Faundez, Gary J. Bassell

gary.bassell@emory.edu

HIGHLIGHTS

Inhibition of Cdh1-APC decreases protein synthesis in cortical neurons

Cdh1 interacts with translational machinery including stress granule proteins

Cdh1-APC regulates the formation of stress granules in neurons through FMRP

Cdh1-APC has a dual role in protein homeostasis

Valdez-Sinon et al., iScience *23*, 101132
May 22, 2020
https://doi.org/10.1016/j.isci.2020.101132

iScience

CellPress
OPEN ACCESS

Article

Cdh1-APC Regulates Protein Synthesis and Stress Granules in Neurons through an FMRP-Dependent Mechanism

Arielle N. Valdez-Sinon,[1] Austin Lai,[1] Liang Shi,[1] Carly L. Lancaster,[1] Avanti Gokhale,[1] Victor Faundez,[1] and Gary J. Bassell[1,2,*]

SUMMARY

Maintaining a balance between protein degradation and protein synthesis is necessary for neurodevelopment. Although the E3 ubiquitin ligase anaphase promoting complex and its regulatory subunit Cdh1 (Cdh1-APC) has been shown to regulate learning and memory, the underlying mechanisms are unclear. Here, we have identified a role of Cdh1-APC as a regulator of protein synthesis in neurons. Proteomic profiling revealed that Cdh1-APC interacts with known regulators of translation, including stress granule proteins. Inhibition of Cdh1-APC activity caused an increase in stress granule formation that is dependent on fragile X mental retardation protein (FMRP). We propose a model in which Cdh1-APC targets stress granule proteins, such as FMRP, and inhibits the formation of stress granules, leading to protein synthesis. Elucidation of a role for Cdh1-APC in regulation of stress granules and protein synthesis in neurons has implications for how Cdh1-APC can regulate protein-synthesis-dependent synaptic plasticity underlying learning and memory.

INTRODUCTION

Spatiotemporal control of protein synthesis and protein degradation at the synapse is required for learning and memory, including long-term potentiation (LTP) and long-term depression (LTD) (Abraham and Williams, 2008; Fonseca et al., 2006; Hou et al., 2006; Karpova et al., 2006; Kauderer and Kandel, 2000). Dysregulated protein homeostasis as a key pathogenic mechanism is implicated in several neurodevelopmental disorders, including Angelman syndrome (Greer et al., 2010; Kishino et al., 1997; Lee et al., 2014), autism spectrum disorders (Tastet et al., 2015; Tsai et al., 2012; Yi et al., 2015), and fragile X syndrome (Gross and Bassell, 2012; Gross et al., 2010; Sharma et al., 2010). Thus, it is crucial that neurons tightly regulate protein turnover at synapses via both the synthesis and degradation of proteins.

Neurons regulate protein content via the ubiquitin-proteasome system (UPS), which drives protein degradation by recognition of ubiquitin modifications and degradation by the 26S proteasome. The attachment of ubiquitin onto a substrate is accomplished by the activity of three classes of enzymes, with E3 ubiquitin ligases being the final enzyme to catalyze the addition of ubiquitin onto a substrate. E3 enzymes have a high specificity for which proteins they will ubiquitinate (David et al., 2011; Hegde, 2004). These enzymes are critical to normal CNS function, and neurological-disease-causing mutations have been found in 13% of known E3 ubiquitin ligase genes (George et al., 2018).

The anaphase-promoting complex, an E3 ubiquitin ligase, and its Cdh1 (also known as Fzr1) regulatory subunit (Cdh1-APC) have been identified to regulate axonal growth (Konishi et al., 2004) and forms of learning and memory (Huang et al., 2015; Pick et al., 2012, 2013). Because this E3 ligase complex has classically been studied in the context of cell-cycle progression (Sudakin et al., 1995), more recent work on Cdh1-APC in differentiated postmitotic neurons has suggested a new role of Cdh1-APC in neurodevelopment (Stegmuller and Bonni, 2005). Although the molecular mechanisms underlying regulation of LTP by Cdh1-APC are unclear (Pick et al., 2012, 2013), the interaction of Cdh1 with the fragile X mental retardation protein (FMRP) was shown to be necessary for mGluR-LTD (Huang et al., 2015). These studies suggest a potential role of Cdh1 to regulate protein synthesis necessary for synaptic plasticity underlying learning and memory. However, a possible role of Cdh1 in protein synthesis in any cell type has not been directly shown. Here we test

[1]Department of Cell Biology, Emory University School of Medicine, Atlanta, GA, 30322, USA

[2]Lead Contact

*Correspondence: gary.bassell@emory.edu

https://doi.org/10.1016/j.isci.2020.101132

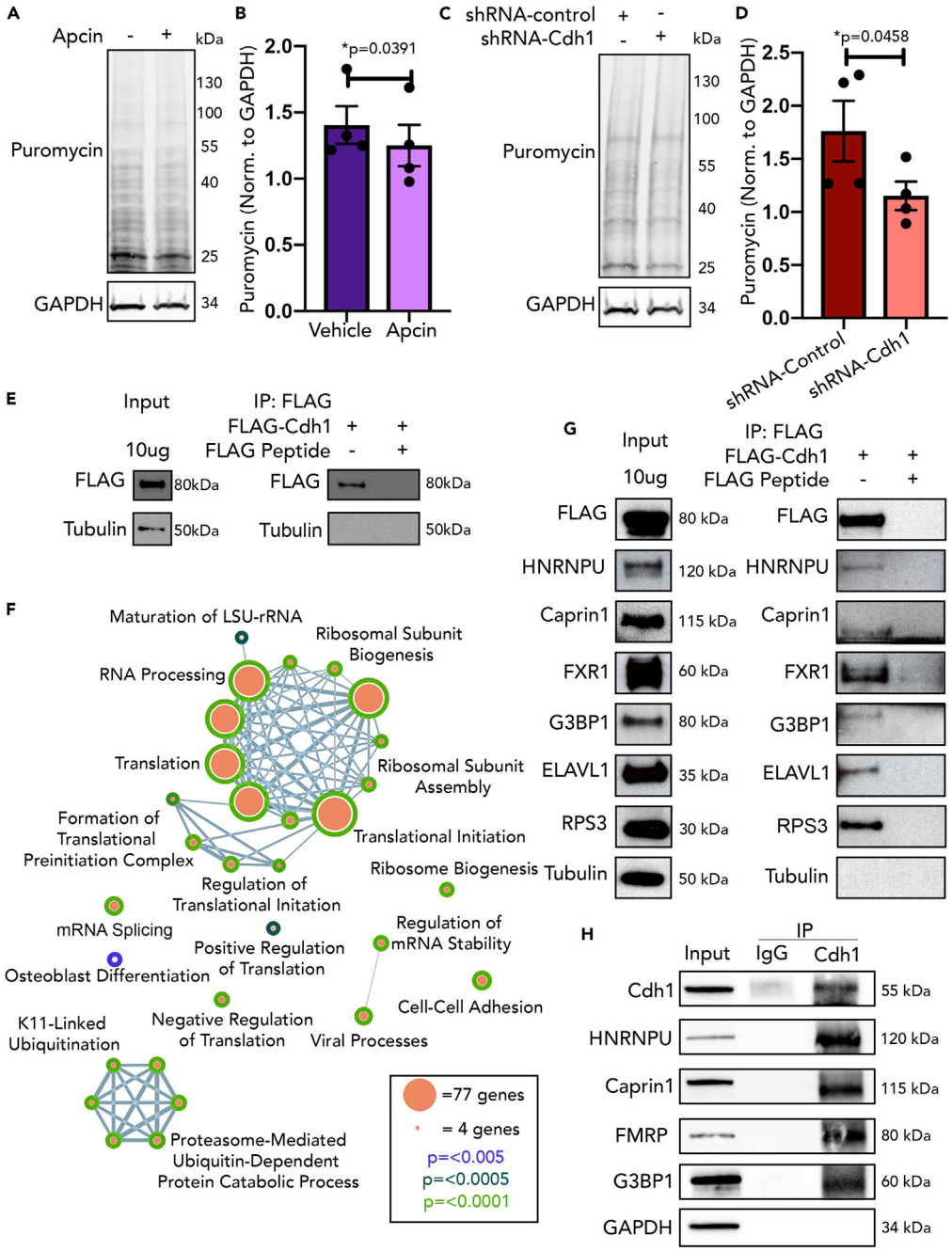

Figure 1. Cdh1-APC Regulates Protein Synthesis in Primary Cortical Neurons and Interacts with Translational Machinery

(A) DIV 14 cortical neurons were treated with Apcin (2μM) for 16–18 h and underwent puromycylation (10μg/mL) for 75 min.

(B) Quantification of puromycin normalized to GAPDH for (A); n = 4.

(C) DIV 7 cortical neurons were transduced with lentivirus expressing shRNA against either Cdh1 or against a control sequence. At DIV 14, neurons underwent puromycylation (10μg/mL) for 75 min.

(D) Quantification of puromycin normalized to GAPDH for (C); n = 4.

(E) N2A cells were transfected with FLAG-Cdh1. Lysate was incubated with immunomagnetic beads coupled to FLAG antibody either in the absence or presence of antigenic 3x FLAG peptide. Chemiluminescent Western blotting demonstrates an enrichment of FLAG-Cdh1.

Figure 1. *Continued*
(F) DAVID biological processes GO-term analysis following mass spectrometry. Size of the nodes indicates number of proteins in the Cdh1 interactome within a specific biological process category. The color of the border of each of the nodes represents the p value as generated by the DAVID analysis.
(G) Stress granule proteins were confirmed to interact with Cdh1 in N2A cells by Western blot analysis following the immunoprecipitation of FLAG-Cdh1; n = 3.
(H) The interactions of stress granule proteins with endogenous Cdh1 in mouse embryonic brain tissue were confirmed by immunoprecipitation and immunoblotting; n = 2.
Data are represented as mean ± SEM. Significance calculated by Student's t test (B, D). See also Tables S1 and S2 and Figure S1.

the hypothesis that Cdh1-APC activity modulates protein synthesis and interacts with translational machinery in addition to its classical role in protein degradation.

In this study, we find that Cdh1-APC can regulate basal protein synthesis, likely through an interaction with translational regulatory proteins. Through an unbiased mass spectrometry screen, it was unexpectedly revealed that Cdh1-APC associates with stress granule proteins including RNA-binding proteins, translational factors, and ribosomal subunits. As stress granules are known to stall translation, the association between Cdh1-APC and stress granules suggests a convergent mechanism by which Cdh1-APC can increase protein synthesis by antagonism of stress granules. Thus, we propose a model in which Cdh1-APC targets key stress granule proteins and inhibits the formation of stress granules, and perhaps other types of RNA granules, leading to increases in protein synthesis. The roles of E3 ubiquitin ligases in protein synthesis and stress granule formation have previously been unclear, and here we show that Cdh1-APC converges on both of these biological processes.

RESULTS

Cdh1-APC Modulates Basal Protein Synthesis

Cdh1-APC has been observed to interact with and ubiquitinate FMRP (Huang et al., 2015), an RNA-binding protein known to repress the translation of mRNAs critical for synaptic structure and function (Darnell et al., 2011). Ubiquitination of FMRP has been proposed as a molecular switch to reverse the repression of protein synthesis by FMRP (Nalavadi et al., 2012), and thus, regulation of an FMRP by Cdh1-APC suggests a potential link between Cdh1-APC and protein synthesis. In addition, a previous study demonstrated that genetic reduction of Cdh1 leads to reduced expression of mGluR-LTD (Huang et al., 2015). Because mGluR-LTD requires new protein synthesis (Kauderer and Kandel, 2000), it is possible that Cdh1-mediated alterations of LTD are due to changes in protein synthesis. Based on these findings, we hypothesized that Cdh1-APC activity regulates protein synthesis in neurons and sought to identify potential molecular mechanisms involved.

To measure steady-state protein synthesis, puromycylation was utilized wherein cells are treated with puromycin and then lysed and immunoblotted for puromycin. Puromycin has structural similarity to aminoacylated tRNA and causes formation of puromycylated nascent peptide chains (David et al., 2012). Cdh1-APC activity was pharmacologically inhibited in day *in vitro* (DIV) 14–16 mouse cortical neurons cells with Apcin (2μM) for 16–18 h (Sackton et al., 2014) (Figure 1A). Apcin-treated neurons demonstrated a reduced signal of puromycin as compared with controls, suggesting that inhibition of Cdh1-APC indeed leads to a decrease in protein synthesis (Figures 1B and S4). This result supports the hypothesis that Cdh1-APC has a function as positive regulator of protein synthesis. In another approach, Cdh1 was genetically knocked down in cortical neurons using a lentivirus expressing shRNA against Cdh1 (Figure S1A); neurons then underwent puromycylation at DIV 14–16 (Figure 1C). Similar to pharmacologic inhibition of Cdh1-APC, knockdown of *Cdh1* (*Fzr1*) led to a significant reduction in protein synthesis (Figures 1D and S4). The observation of decreased protein synthesis in postmitotic cortical neurons suggests that the inhibitory effects of Cdh1-APC on protein synthesis are independent of its role in mitotic cells. Apcin has been shown to act more selectively on APC with its other regulatory subunit, Cdc20 (Cdc20-APC), compared with Cdh1-APC (Sackton et al., 2014). To utilize another form of pharmacologic inhibition against Cdh1-APC, neurons were treated with proTAME, which is more selective for Cdh1-APC than Cdc20-APC (Sackton et al., 2014) (Figure S1B). Puromycylation following proTAME treatment demonstrated a trend toward a decrease in protein synthesis (Figures S1C and S4), which suggests that changes in protein synthesis following Apcin treatment may be partially due to Cdc20-APC-mediated mechanisms in addition to Cdh1-APC. However, the significant reduction in protein synthesis following Cdh1 knockdown supports the hypothesis that

Cdh1-APC regulates protein synthesis. The role of Cdh1-APC in regulation of protein synthesis has not been investigated previously in any cell type, and this finding demonstrating that Cdh1-APC can regulate protein synthesis sheds light on a potential function of the Cdh1-APC complex in postmitotic neurons.

The Cdh1-APC Interactome Is Enriched with Regulators of Protein Synthesis

Following observations of a role of Cdh1-APC in protein synthesis, we sought to identify factors involved in a mechanism by which Cdh1-APC may regulate protein synthesis. As FMRP has already been identified as an interactor and substrate of Cdh1-APC E3 ligase activity (Huang et al., 2015), we investigated whether Cdh1-APC interacts with other RNA binding proteins known to regulate translation. To take an unbiased approach in identifying other Cdh1-interactors, Neuro2A (N2A) cells were transfected with FLAG-Cdh1 and lysates underwent FLAG-immunoaffinity chromatography with FLAG-peptide elution (Figure 1E) (Comstra et al., 2017; Gokhale et al., 2012). A portion of the lysate was co-incubated with FLAG peptide to outcompete FLAG-Cdh1 and allow for identification of nonspecific binding proteins to bead-antibody complexes. Following confirmation of sufficient protein pulldown with silver staining (Figure S1D), the immunoprecipitate was analyzed by mass spectrometry. The Cdh1 interactome included 185 unique proteins (Table S1). Not surprisingly, the interactome included known components of the Cdh1-APC complex, such as APC1, APC2, APC7, CDC16, CDC23, and CDC27. Enrichment of APC subunits validated the specificity of the FLAG-immunoaffinity purification. A DAVID analysis was then conducted to identify enriched biological processes among interactome components (Table S2). Aside from expected enrichment in categories related to the ubiquitin-proteasome system such as protein K11-linked ubiquitination (GO:00709791, $p = 7.57 \times 10^{-6}$), the interactome was highly enriched in categories related to protein synthesis (Figure 1F, Table S2). Of interest, 36.7% of the Cdh1 interactome was categorized into translation (GO:0006412, $p = 4.09 \times 10^{-73}$). Other translation-related biological processes that were enriched in the Cdh1 interactome include formation of translation preinitiation complex (GO:0001731, $p = 8.07 \times 10^{-13}$), regulation of translational initiation (GO:0006446, $p = 2.22 \times 10^{-12}$), positive regulation of translation (GO:0045727, $p = 2.16 \times 10^{-4}$), negative regulation of translation (GO:0017148, $p = 1.39 \times 10^{-7}$), and ribosomal subunit assembly (GO:0000027, $p = 7.76 \times 10^{-12}$; GO:0000028, $p = 2.05 \times 10^{-11}$). The significant enrichment of proteins involved in translational processes supports a role of Cdh1-APC in translation regulation outside of its canonical roles in ubiquitination and cell cycle.

Cdh1-APC Interacts with Stress Granule Proteins

Interestingly, mass spectrometry identified that Cdh1 interacts with one of the FMRP autosomal homologs, FXR1. FMRP and FXR1 have been shown to interact and form cytoplasmic RNA granules that have the ability to repress the translation of mRNA (Gareau et al., 2013; Mazroui et al., 2002). These RNA granules are referred to as fragile X granules (FXG) and are found in neurons (Christie et al., 2009) and have similar properties to stress granules. Based on observed interactions of Cdh1 with FMRP (Figure 1H) (Huang et al., 2015) and FXR1 (Figures 1G and 1H), we aimed to elucidate if there is a broader connection between Cdh1 and stress granules. The association of FMRP with stress granules has been shown previously (Didiot et al., 2009; Markmiller et al., 2018). We compared our Cdh1-interactome with previously published lists of stress granule proteins (Jain et al., 2016; Markmiller et al., 2018) and found that the Cdh1-interactome was highly enriched for stress granule proteins (28% of the Cdh1 interactome) (Table S1). We confirmed that the established stress granule proteins HNRNPU, Caprin1, G3BP1, ELAVL1, and RPS3 interact with Cdh1 using immunoprecipitation and immunoblotting (Figure 1G). By a similar strategy, the interactions of stress granule proteins G3BP1, HNRNPU, Caprin 1, and FMRP with endogenous Cdh1 were confirmed in mouse embryonic brain tissues (Figure 1H). As it has been well described that stress granules can stall the translation of mRNA (Protter and Parker, 2016), we hypothesized that Cdh1-APC can regulate protein synthesis through the control of stress granule dynamics.

Stress Granule Formation Reduces Protein Synthesis

As a model system to investigate the interplay between protein synthesis and RNA granules, the sodium arsenite paradigm ($NaAsO_2$) was used to stimulate stress granule formation (Markmiller et al., 2019). As our hypothesis that Cdh1-APC regulates protein synthesis through stress granule formation is dependent on the ability of stress granules to repress protein synthesis, we first needed to confirm that stress granule formation following $NaAsO_2$ treatment leads to a decrease in protein synthesis. N2A cells (Figures 2A and S4) and DIV 14 cortical neurons (Figures 2C and S4) were treated with $NaAsO_2$ (0.5mM) or water as a control for 45 min and concurrently underwent puromycin labeling. Upon immunoblotting for puromycin, there was a substantial decrease in protein synthesis with $NaAsO_2$ treatment (Figures 2B and 2D). The decrease

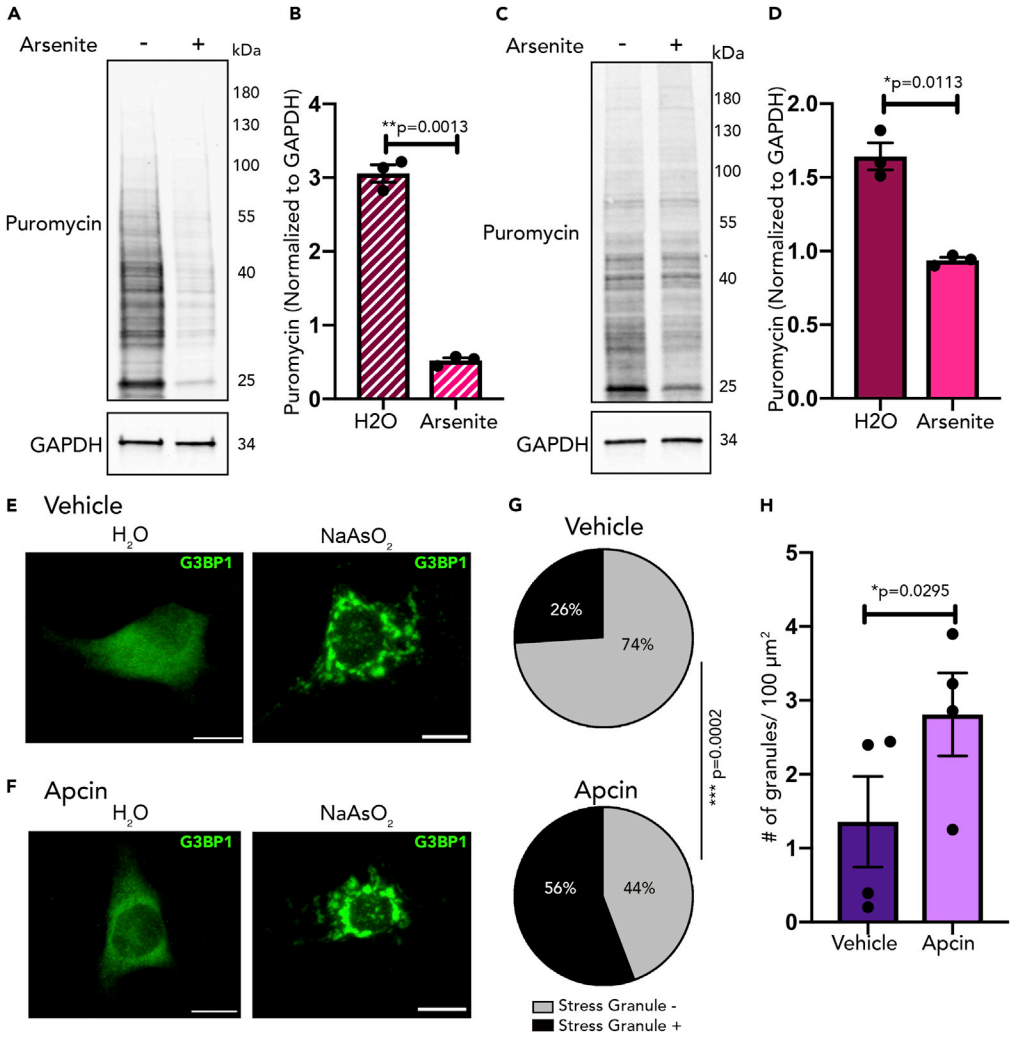

Figure 2. Stress Granule Formation Inhibits Protein Synthesis and Is Regulated by Cdh1-APC

(A) N2A cells underwent puromycin labeling following 45 min of treatment with sodium arsenite or water. Lysates were immunoblotted for puromycin and GAPDH.

(B) Quantification of puromycin normalized to GAPDH from (A); n = 3.

(C) DIV 14 cortical neurons underwent puromycin labeling following 75 min of treatment with sodium arsenite or water. Lysates were immunoblotted for puromycin and GAPDH.

(D) Quantification of puromycin normalized to GAPDH from (C); n = 3.

(E and F) DIV 14 cortical neurons were treated with vehicle (DMSO) or Apcin for 16–18 h. Neurons were then treated with sodium arsenite ($NaAsO_2$) (0.5mM) or water for 45 min prior to fixation. Immunofluorescence was done with antibodies against G3BP1. Scale bar indicates 10µM.

(G) User-blind scoring of neurons that were stress-granule-positive or stress-granule-negative following arsenite treatment; n = 73 neurons for vehicle, 78 neurons for Apcin.

(H) Quantification of number of stress granules in the soma per 100 μm^2; n = 4.

Data are represented as mean ± SEM. Statistical significance was calculated by Student's t test (B, D, and H) and Z test (G).

in protein synthesis concomitant with stress granule formation suggests that stress granule dynamics may be a potential convergent mechanism by which Cdh1-APC may regulate protein synthesis.

Cdh1-APC Regulates Stress Granule Formation

Following observations that inhibition of Cdh1-APC leads to a decrease in protein synthesis, we hypothesized that this translational repressive state may be due to favored formation of RNA granules. DIV 15

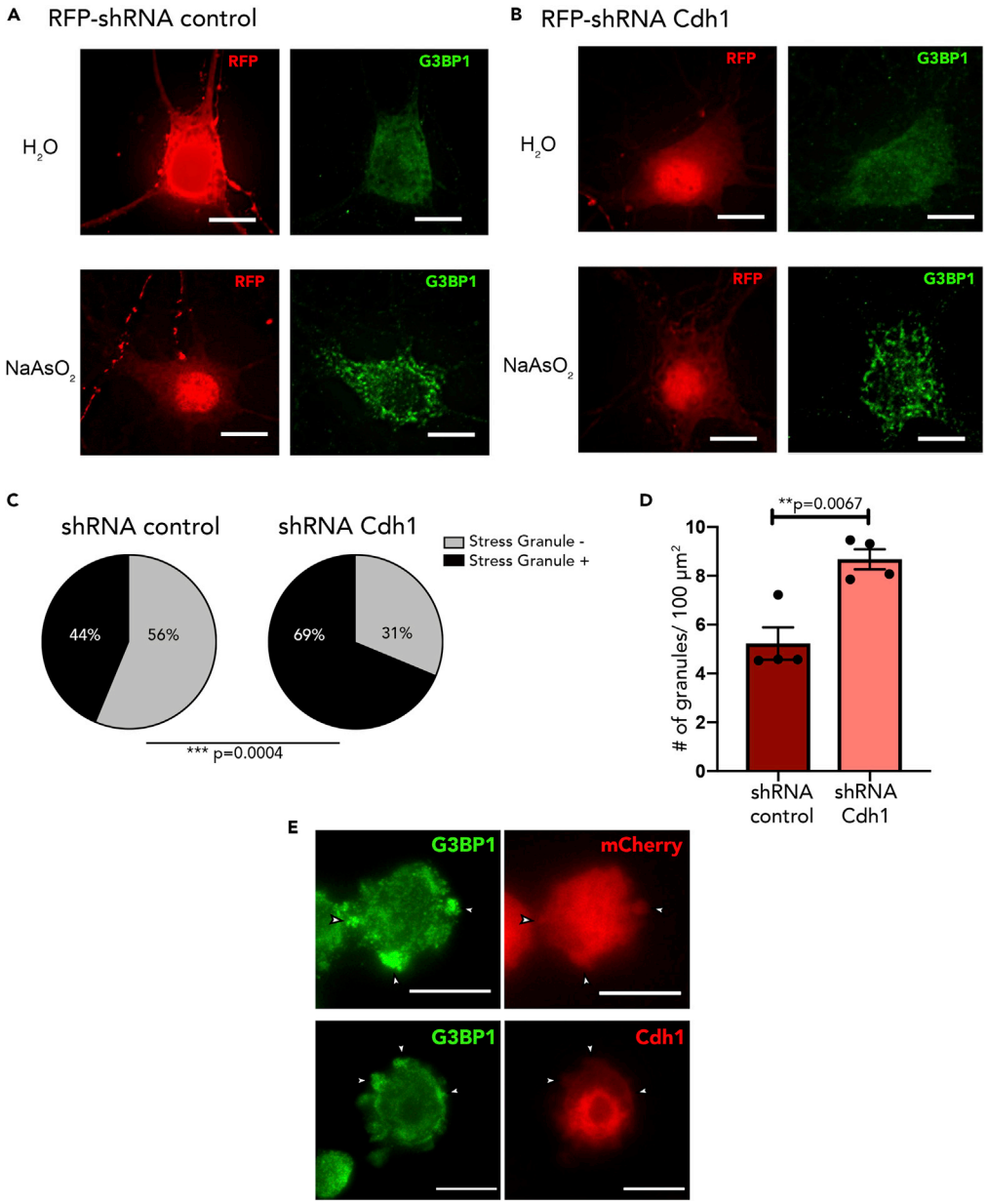

Figure 3. Knockdown of Cdh1-APC Promotes Stress Granule Formation

(A and B) DIV 7 neurons were transduced with lentivirus expressing RFP-tagged non-targeting construct (A) or RFP-tagged shRNA against Cdh1 (B). At DIV 14, neurons were then treated with sodium arsenite and immunostained as described above. Scale bar indicates 10µm.

(C) User-blind scoring of neurons that were stress-granule-positive or stress-granule-negative following arsenite treatment; n = 80 neurons for both groups.

(D) Quantification of number of stress granules in the soma per 100 μm^2; n = 4.

(E) Neuro2A cells were transfected with mCherry or mCherry-Cdh1. Cells were treated with sodium arsenite for 45 min to induce stress granules and then fixed in 4% paraformaldehyde and then immunostained for G3BP. Arrows indicate stress granule accumulation. Scale bar represents 10µm.

Data are represented as mean ± SEM. Statistical significance was calculated by Z test (C) and Student's t test (D).

mouse cortical neurons were treated with $NaAsO_2$ (0.5mM, 45 min) and immunostained for G3BP1, an interactor of Cdh1 that we identified in the Cdh1 interactome and known stress granule protein (Jain et al., 2016; Markmiller et al., 2018). Control and Apcin-treated neurons form stress granules upon sodium

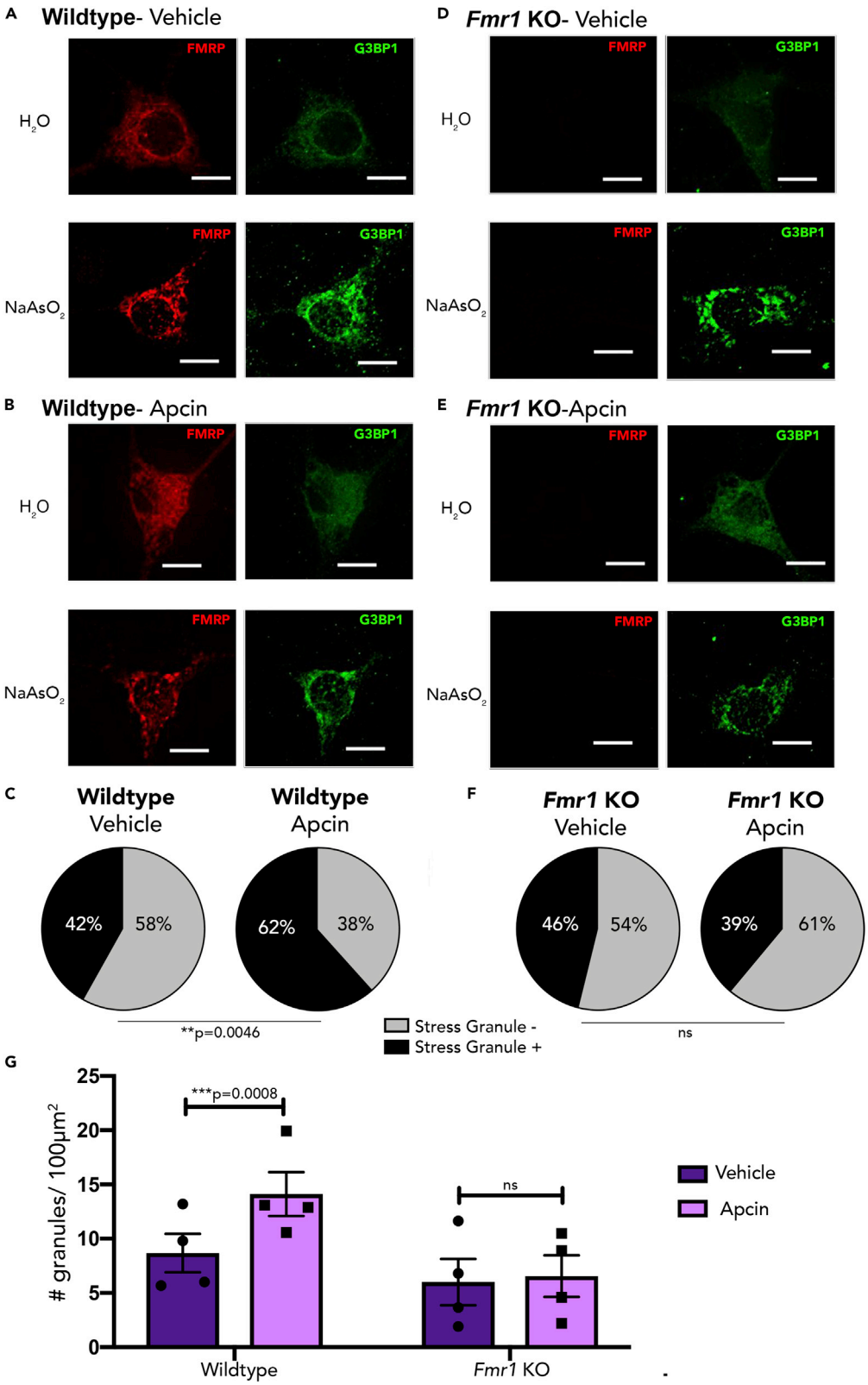
A
Wildtype- Vehicle
FMRP
G3BP1
H2O
NaAsO2
D
Fmr1 KO- Vehicle
B
Wildtype- Apcin
E
Fmr1 KO-Apcin
C
Wildtype
Vehicle
Wildtype
Apcin
42%
58%
62%
38%
**p=0.0046
F
Fmr1 KO
Vehicle
Fmr1 KO
Apcin
46%
54%
39%
61%
ns
Stress Granule -
Stress Granule +
G
granules/ 100µm2
***p=0.0008
ns
Vehicle
Apcin
Wildtype
Fmr1 KO

Figure 4. Cdh1-APC Regulates Stress Granule Dynamics via an FMRP-Dependent Mechanism

(A and B) Postnatal wild-type DIV 14–16 cortical neurons were treated with vehicle (DMSO) (A) or Apcin (B) for 16–18 hr. Neurons were then treated with sodium arsenite and immunostained with antibody to G3BP1. Scale bar indicates 10μm.

(C) Quantification of stress granule negative or positive cells; n = 74 cells for Vehicle-treated and 73 cells for Apcin-treated.

(D and E) Postnatal *Fmr1*-knockout (KO) DIV 14–16 cortical neurons were treated with vehicle (DMSO) (D) or Apcin (E) for 16–18 h and treated with sodium arsenite and fixed as described above.

(F) Quantification of stress-granule-negative or -positive cells; n = 78 cells for Vehicle-treated and 77 cells for Apcin-treated.

(G) Quantification of number of stress granules in the soma per 100 μm^2 for all four conditions; n = 4.

Data are represented as mean ± SEM. Statistical significance was calculated by Z test (C and F) and two-way ANOVA (G).

arsenite treatment (Figures 2E and 2F). When comparing stress granules in both sets of neurons, the percentage of stress granule positive neurons was significantly greater in the Apcin-treated neurons compared with the control neurons (Figure 2G). Although only 26% of control neurons formed stress granules, 56% of Apcin-treated neurons were stress-granule-positive after arsenite treatment. In addition, there were significantly more stress granules in the soma of Apcin-treated cells compared with vehicle-treated cells (Figure 2H). These results link inhibition of Cdh1-APC activity to increased stress granule formation.

To confirm our findings that Cdh1-APC regulates stress granule formation, Cdh1-APC was also inhibited pharmacologically with proTAME (Figure S2) or with shRNA knockdown (Figures 3A–3D). Both alternative approaches of inhibiting Cdh1-APC lead to a significant increase in the percentage of cells forming stress granules (Figures 3C and S2B) and an increase in the number of stress granules in the soma (Figures 3D and S2C). These data demonstrate that Cdh1-APC has a previously unexplored role in the regulation of stress granules through its ability to antagonize the formation of stress granules.

Cdh1-APC Regulates Stress Granules in an FMRP-Dependent Mechanism

Although Cdh1-APC activity impacts stress granule formation, we did not observe that Cdh1 co-localizes with stress granules (Figure 3E); Cdh1 has also not been identified as a stress granule protein (Jain et al., 2016; Markmiller et al., 2018). This suggests that although Cdh1-APC interacts with stress granule proteins perhaps in a transient and dynamic manner, it is not an integral component of stress granule. Thus, Cdh1-APC may be affecting stress granule formation through its interaction with and modification of stress granule proteins. With previous literature identifying that FMRP is a ubiquitination target of Cdh1-APC (Huang et al., 2015) and is involved in stress granule formation (Didiot et al., 2009), we hypothesized that the regulation of stress granules by Cdh1-APC is FMRP dependent.

To explore how interaction with FMRP may affect Cdh1-mediated regulation of stress granule formation, cortical neurons from *Fmr1*-KO mice, a model of Fragile X syndrome, and wild-type littermates underwent treatment with Apcin and sodium arsenite to induce stress granule formation (Figures 4A, 4B, 4D, and 4E). Similar to previous experiments, Apcin treatment increased the formation of stress granules in wild-type cortical neurons (Figures 4C and 4G). However, Apcin treatment did not elicit any changes in the formation of stress granules in *Fmr1*-KO neurons (Figures 4F and 4G). Thus, Apcin-induced changes in stress granule formation require FMRP. Inability to increase the formation of stress granules in *Fmr1*-KO neurons supports our hypothesis that FMRP is necessary for Cdh1-APC to regulate stress granule formation. Further work is needed to more fully understand how the full scope of molecular interactions between FMRP and other Cdh1-associated factors identified in this study regulate stress granules by ubiquitination.

Taken together, these findings demonstrate a convergent role of Cdh1-APC to regulate stress granule formation and protein synthesis in neurons. Furthermore, we link the function of Cdh1-APC as a translational regulator to its interaction with FMRP, a protein linked to synapse development and function.

DISCUSSION

Regulation of Stress Granules by Cdh1-APC

Here we demonstrate a role of Cdh1-APC in stress granule assembly. The role of specific E3 ligases to regulate stress granules has not been shown. Stress granules are membraneless organelles that recruit and repress translation of mRNAs in response to various stressors that include arsenite, heat shock, and oxidative stress (Buchan and Parker, 2009; Protter and Parker, 2016). Altered stress granule formation

and dynamics have gained considerable attention in some neurological diseases, such as mutations of RNA-binding proteins that cause amyotrophic lateral sclerosis (Li et al., 2013; Monahan et al., 2016). A better understanding of the role of Cdh1-APC role in stress granule formation may provide insights into how to ameliorate altered stress granule dynamics in neurological disorders.

Recent studies have provided conflicting reports on the role of ubiquitination in stress granule dynamics. In two studies, manipulation of the ubiquitin proteasome system (UPS) did affect stress granule formation (Mazroui et al., 2007; Xie et al., 2018). However, in a recent study, pharmacologic inhibition of the E1 ubiquitin-activating enzyme did not affect stress granule assembly or disassembly, suggesting that active conjugation of ubiquitin does not regulate stress granule formation (Markmiller et al., 2019). These prior studies used methods that would broadly impact UPS. Our data show that Cdh1-APC, a well-known E3 ubiquitin ligase, indeed regulates stress granule formation. Another possible reason for the differences in our observation of UPS function in stress granule formation is cell-type specificity. Although our study used neurons, previous work utilized HeLa and 293T HEK cells, which are both non-neuronal cell lines. It is possible that our observed phenotypes of stress granule and protein synthesis regulation by Cdh1-APC may only occur in neural-lineage cell types. Furthermore, a previous study demonstrated that there are cell-specific changes in the stress granule interactome, with neurons having the most diverse stress granule interactome (Markmiller et al., 2018). Interestingly, the neuron stress granule interactome is enriched with quality control factors (Markmiller et al., 2018). As the UPS is involved in cell quality control, this previous evidence supports our findings that an E3 ubiquitin ligase regulates neuronal stress granule dynamics. Thus, our data taken together with previous work suggest that Cdh1-APC and the UPS may play a cell-type-specific role that contributes to additional spatiotemporal control of protein homeostasis that is critical in neural cells.

Stress granule proteins interact in a pre-existing network in unstressed conditions, and the stress stimulus causes the formation of the stress granules (Markmiller et al., 2018). The dynamic ability of the stress granule protein network to quickly respond to stress suggests modifying events that include posttranslational modifications. It is likely that there are antagonistic modifications that regulate the dynamics between assembly and disassembly. Our data suggest that ubiquitination is a molecular switch to antagonize stress granule formation. Thus, our working model is that Cdh1-APC modifies (presumably by ubiquitinating) stress granule proteins, making them less efficiently incorporated into stress granules and supporting protein synthesis.

The present study utilizes stress granules induced by sodium arsenite treatment as a model mRNP granule. As there are many other forms of mRNP granules such as processing bodies (PBs) and RNA transport granules, our work may have implications for these other diverse RNA granules. The Cdh1 interactome includes proteins that are involved in RNA transport granules in addition to stress granules, such as FMRP (Antar et al., 2004; Dictenberg et al., 2008) and Caprin (Nakayama et al., 2017; Shiina et al., 2010). With an underlying shared biology among RNA granules, Cdh1-APC may also regulate assembly or disassembly of mRNA transport granules, FX granules, or PBs and their translational control at synapses. Thus, a next step in the research on Cdh1-APC should be to elucidate if Cdh1-APC regulates PBs and/or mRNA transport granules in addition to stress granules as observed in this study.

Cdh1-APC Modification of FMRP

Although Cdh1 has been observed to have APC-independent functions (Wan et al., 2011), our observations with Apcin, a well-described APC inhibitor (Sackton et al., 2014), support a model in which APC catalytic activity is necessary for Cdh1-mediated changes in stress granule formation and protein synthesis. Although it is unknown if Cdh1-APC directly ubiquitinates the interacting stress granule proteins identified in this study, it has been demonstrated that Cdh1-APC ubiquitinates FMRP, a known component that regulates stress granules. Preventing Cdh1-APC interaction with FMRP may increase translational repression through the formation of stress granules. It is also likely that Cdh1-APC is able to modify other stress granule proteins to regulate this process. Treatment with sodium arsenite does not change expression levels of FMRP or Cdh1 (Figure S3), which further supports the hypothesis that modifications and dynamics between these two proteins are responsible for changes downstream of sodium arsenite treatment.

It is still unclear how ubiquitination of FMRP by Cdh1-APC impacts its ability to form stress granules. One possibility is that ubiquitination of FMRP leads to its degradation by the proteasome, and its

absence prevents the formation of stress granules. A previous study demonstrated that loss of FMRP disrupts stress granule formation, potentially due to its aggregation properties (Didiot et al., 2009). Thus, it is most likely that the degradation of FMRP following ubiquitination by Cdh1-APC mediates the changes in stress granule dynamics. However, another possibility is that the ubiquitination of FMRP elicits downstream signaling that causes a dynamic change in the stress granule proteome that is independent of FMRP degradation. Further investigation of how FMRP shuttling between diverse granules and polyribosomes is altered following ubiquitination will be necessary to better understand how Cdh1-APC can carry out changes in protein synthesis. Elucidation of this mechanism can be utilized to identify points of pathophysiology in forms of neurodevelopmental disorders that are characterized by dysregulated protein synthesis and/or disrupted ubiquitination pathways.

Potential Dual Roles of Cdh1-APC

Although Cdh1-APC has been long considered to contribute to degradation of proteins via its role as an E3-ubiquitin ligase, its role in regulating protein synthesis has been overlooked prior to this study. From this work, it could be proposed that Cdh1-APC has dual roles in the neural cell: to ubiquitinate proteins in order to enhance the degradation processes and to promote protein synthesis through the antagonism of stress granules. However, it is possible that these two roles of Cdh1-APC are synergistic to ultimately increase protein synthesis in the cell. For example, the ability for Cdh1-APC to antagonize the formation of stress granules may be completely dependent on its ability to ubiquitinate stress granule proteins, such as FMRP. To distinguish whether Cdh1-APC has two distinct roles in protein degradation and synthesis or if Cdh1-APC-mediated ubiquitination is necessary to elicit changes in protein synthesis, there needs to be further characterization of signals that enhance or inhibit Cdh1-APC activity in neurons. For example, as it is established that mGluR signaling enhances downstream ubiquitination of proteins by Cdh1-APC (Huang et al., 2015), it will be of interest to determine whether mGluR signaling contributes to Cdh1-APC-mediated changes in stress granule formation. Better understanding of the upstream regulation of Cdh1-APC will help to better understand the extent by which Cdh1-APC can affect protein degradation and synthesis and whether or not these are synergistic or distinct processes.

Limitations of the Study

Although our study highlights that Cdh1-APC interacts with stress granule proteins, it is unclear whether or not Cdh1-APC ubiquitinates these proteins. A future focus will be to better understand the consequences of Cdh1-APC interactions with stress granule proteins, translational initiation factors, and ribosomal subunits that we identified through mass spectrometry. Cdh1-APC has been characterized to lead to the degradation of its ubiquitination targets following polyubiquitination on the K11 residue of ubiquitin (Budhavarapu et al., 2012). Therefore, Cdh1-APC may be targeting these translational regulatory proteins for degradation via K11-linked polyubiquitination. However, ubiquitination can lead to fates other than degradation. For example, K63-linked polyubiquitination can cause DNA repair (Liu et al., 2018), endocytosis (Lauwers et al., 2009), or NF-kB activation (Deng et al., 2000). It is possible that ubiquitination by Cdh1-APC of stress granule proteins, ribosomes, and initiation factors can lead to noncanonical pathways aside from degradation. A vital future direction of this work is to determine the fate of Cdh1-APC ubiquitination targets.

Conclusions

We have uncovered that Cdh1-APC is a regulator of protein synthesis in mature cortical neurons. Inhibition of Cdh1-APC activity leads to a decrease in protein synthesis in postmitotic cortical neurons, demonstrating a role for Cdh1-APC independent of its characterized roles in mitotic cells. Proteomic profiling revealed that the Cdh1 interactome is highly enriched in translational regulatory proteins and stress granule proteins. Stress granule formation leads to decreases in protein synthesis, and we observe that Cdh1-APC activity regulates stress granule assembly in cortical neurons; these effects are meditated by interaction of Cdh1-APC with FMRP. In *Fmr1-KO* neurons, stress granule formation is impaired, and neurons are insensitive to perturbation of Cdh1. This suggests a potential key role of FMRP interactions with Cdh1-APC in not only the ubiquitination of FMRP itself (Huang et al., 2015) but also many of the associated translational factors, ribosomal proteins, and RNA binding proteins identified in the Cdh1 interactome. Thus, we propose a model in which Cdh1-APC activity antagonizes the formation of stress granules via interaction with FMRP, which allows for increases in protein synthesis. Although FMRP is a necessary key player, further work is needed to broadly understand the mechanistic role of the FMRP destruction box motif (Huang et al.,

2015) to recruit Cdh1 and potentially other Cdh1-interactors to regulate stress granules via a shared ubiquitination signaling pathway.

Our data indicate a dual role of Cdh1-APC in protein homeostasis—it is able to reduce the level of proteins through its role in tagging substrates for degradation by the proteasome and also can lead to an increase in protein synthesis through its antagonism of stress granule formation. Elucidation of the role of Cdh1-APC in protein synthesis and regulation of translational proteins, such as FMRP, in postmitotic neurons will broaden the understanding of protein homeostasis at the synapse that is vital for protein-synthesis-dependent synaptic plasticity underlying learning and memory.

These findings are expected to uncover new and broader relationships between Cdh1-APC and diverse types of RNA granules relevant to protein-synthesis-dependent regulation of synapse function. For example, Cdh1-APC regulates changes in protein synthesis necessary for molecular forms of learning, such as mGluR-LTD previously demonstrated to be downstream of Cdh1-APC signaling (Huang et al., 2015). Our findings of an interplay between protein synthesis and stress granules have implications to understand how RNA granule hypo-assembly may contribute to neurodevelopmental disorders including those linked to alterations in E3 ligase expression and function, such as Angelman syndrome. It is unlikely that alterations in Cdh1-APC function can be directly targeted for FXS treatment but perhaps other strategies that can restore RNA granule formation.

Resource Availability

Lead Contact

Further information and requests for resources and reagents should be directed to and will be fulfilled by the Lead Contact, Dr. Gary J. Bassell (gary.bassell@emory.edu).

Materials Availability

The mCherry-myc and mCherry-Cdh1-myc plasmids generated in this study will be made available on request, but we may require a payment and/or a completed Materials and Transfer Agreement if there is a potential for commercial application.

Data and Code Availability

The mass spectrometry proteomics data generated in thus study have been deposited to the ProteomeXChange Consortium (Vizcaino et al., 2014) via the PRIDE partner repository (Perez-Riverol et al., 2019) under accession number: PXD018875.

METHODS

All methods can be found in the accompanying Transparent Methods supplemental file.

SUPPLEMENTAL INFORMATION

Supplemental Information can be found online at https://doi.org/10.1016/j.isci.2020.101132.

ACKNOWLEDGMENTS

This work was funded by NIH R01 MH109026 (GJB), F31 NS101932 (ANV), 1R56MH111459 (VF), and 1RF1AG060285 (VF). We thank Pernille Bülow and Nisha Raj for their helpful comments on the manuscript. We also thank Pernille Bülow for providing us with postnatal cortical neurons. We thank Azad Bonni for providing experimental constructs. This study was supported in part by the Emory Integrated Genomics Core (EIGC), the Viral Vector Core of the Emory Neuroscience NINDS Core Facilities grant (P30NS055077), and the National Center for Advancing Translational Sciences of the National Institutes of Health (UL1TR000454).

AUTHOR CONTRIBUTIONS

Conceptualization, experimental design, data analysis, and interpretation were by ANV, VF, and GJB. ANV, AL, and CLL carried out experiments. LS performed stress granule quantification. AG provided methodology and training. VF performed bioinformatic analysis. ANV and GJB contributed to the writing of the manuscript. Lab infrastructure and resources were by GJB and VF.

DECLARATION OF INTERESTS

The authors declare no competing interests.

Received: August 5, 2019
Revised: January 22, 2020
Accepted: April 28, 2020
Published: May 22, 2020

REFERENCES

Abraham, W.C., and Williams, J.M. (2008). LTP maintenance and its protein synthesis-dependence. Neurobiol. Learn. Mem. *89*, 260–268.

Antar, L.N., Afroz, R., Dictenberg, J.B., Carroll, R.C., and Bassell, G.J. (2004). Metabotropic glutamate receptor activation regulates fragile x mental retardation protein and FMR1 mRNA localization differentially in dendrites and at synapses. J. Neurosci. *24*, 2648–2655.

Buchan, J.R., and Parker, R. (2009). Eukaryotic stress granules: the ins and outs of translation. Mol. Cell *36*, 932–941.

Budhavarapu, V.N., White, E.D., Mahanic, C.S., Chen, L., Lin, F.T., and Lin, W.C. (2012). Regulation of E2F1 by APC/C Cdh1 via K11 linkage-specific ubiquitin chain formation. Cell Cycle *11*, 2030–2038.

Christie, S.B., Akins, M.R., Schwob, J.E., and Fallon, J.R. (2009). The FXG: a presynaptic fragile X granule expressed in a subset of developing brain circuits. J. Neurosci. *29*, 1514–1524.

Comstra, H.S., McArthy, J., Rudin-Rush, S., Hartwig, C., Gokhale, A., Zlatic, S.A., Blackburn, J.B., Werner, E., Petris, M., D'Souza, P., et al. (2017). The interactome of the copper transporter ATP7A belongs to a network of neurodevelopmental and neurodegeneration factors. Elife *6*, e24722.

Darnell, J.C., Van Driesche, S.J., Zhang, C., Hung, K.Y., Mele, A., Fraser, C.E., Stone, E.F., Chen, C., Fak, J.J., Chi, S.W., et al. (2011). FMRP stalls ribosomal translocation on mRNAs linked to synaptic function and autism. Cell *146*, 247–261.

David, A., Dolan, B.P., Hickman, H.D., Knowlton, J.J., Clavarino, G., Pierre, P., Bennink, J.R., and Yewdell, J.W. (2012). Nuclear translation visualized by ribosome-bound nascent chain puromycylation. J. Cell Biol. *197*, 45–57.

David, Y., Ternette, N., Edelmann, M.J., Ziv, T., Gayer, B., Sertchook, R., Dadon, Y., Kessler, B.M., and Navon, A. (2011). E3 ligases determine ubiquitination site and conjugate type by enforcing specificity on E2 enzymes. J. Biol. Chem. *286*, 44104–44115.

Deng, L., Wang, C., Spencer, E., Yang, L., Braun, A., You, J., Slaughter, C., Pickart, C., and Chen, Z.J. (2000). Activation of the IkappaB kinase complex by TRAF6 requires a dimeric ubiquitin-conjugating enzyme complex and a unique polyubiquitin chain. Cell *103*, 351–361.

Dictenberg, J.B., Swanger, S.A., Antar, L.N., Singer, R.H., and Bassell, G.J. (2008). A direct role for FMRP in activity-dependent dendritic mRNA transport links filopodial-spine morphogenesis to fragile X syndrome. Dev. Cell *14*, 926–939.

Didiot, M.C., Subramanian, M., Flatter, E., Mandel, J.L., and Moine, H. (2009). Cells lacking the fragile X mental retardation protein (FMRP) have normal RISC activity but exhibit altered stress granule assembly. Mol. Biol. Cell *20*, 428–437.

Fonseca, R., Vabulas, R.M., Hartl, F.U., Bonhoeffer, T., and Nagerl, U.V. (2006). A balance of protein synthesis and proteasome-dependent degradation determines the maintenance of LTP. Neuron *52*, 239–245.

Gareau, C., Martel, D., Coudert, L., Mellaoui, S., and Mazroui, R. (2013). Characterization of fragile X mental retardation protein granules formation and dynamics in Drosophila. Biol. Open *2*, 68–81.

George, A.J., Hoffiz, Y.C., Charles, A.J., Zhu, Y., and Mabb, A.M. (2018). A comprehensive atlas of E3 ubiquitin ligase mutations in neurological disorders. Front. Genet. *9*, 29.

Gokhale, A., Larimore, J., Werner, E., So, L., Moreno-De-Luca, A., Lese-Martin, C., Lupashin, V.V., Smith, Y., and Faundez, V. (2012). Quantitative proteomic and genetic analyses of the schizophrenia susceptibility factor dysbindin identify novel roles of the biogenesis of lysosome-related organelles complex 1. J. Neurosci. *32*, 3697–3711.

Greer, P.L., Hanayama, R., Bloodgood, B.L., Mardinly, A.R., Lipton, D.M., Flavell, S.W., Kim, T.K., Griffith, E.C., Waldon, Z., Maehr, R., et al. (2010). The Angelman Syndrome protein Ube3A regulates synapse development by ubiquitinating arc. Cell *140*, 704–716.

Gross, C., and Bassell, G.J. (2012). Excess protein synthesis in FXS patient lymphoblastoid cells can be rescued with a p110beta-selective inhibitor. Mol. Med. *18*, 336–345.

Gross, C., Nakamoto, M., Yao, X., Chan, C.B., Yim, S.Y., Ye, K., Warren, S.T., and Bassell, G.J. (2010). Excess phosphoinositide 3-kinase subunit synthesis and activity as a novel therapeutic target in fragile X syndrome. J. Neurosci. *30*, 10624–10638.

Hegde, A.N. (2004). Ubiquitin-proteasome-mediated local protein degradation and synaptic plasticity. Prog. Neurobiol. *73*, 311–357.

Hou, L., Antion, M.D., Hu, D., Spencer, C.M., Paylor, R., and Klann, E. (2006). Dynamic translational and proteasomal regulation of fragile X mental retardation protein controls mGluR-dependent long-term depression. Neuron *51*, 441–454.

Huang, J., Ikeuchi, Y., Malumbres, M., and Bonni, A. (2015). A Cdh1-APC/FMRP ubiquitin signaling link drives mGluR-dependent synaptic plasticity in the mammalian brain. Neuron *86*, 726–739.

Jain, S., Wheeler, J.R., Walters, R.W., Agrawal, A., Barsic, A., and Parker, R. (2016). ATPase-modulated stress granules contain a diverse proteome and substructure. Cell *164*, 487–498.

Karpova, A., Mikhaylova, M., Thomas, U., Knopfel, T., and Behnisch, T. (2006). Involvement of protein synthesis and degradation in long-term potentiation of Schaffer collateral CA1 synapses. J.Neurosci. *26*, 4949–4955.

Kauderer, B.S., and Kandel, E.R. (2000). Capture of a protein synthesis-dependent component of long-term depression. Proc. Natl. Acad. Sci. U S A *97*, 13342–13347.

Kishino, T., Lalande, M., and Wagstaff, J. (1997). UBE3A/E6-AP mutations cause Angelman syndrome. Nat. Genet. *15*, 70–73.

Konishi, Y., Stegmuller, J., Matsuda, T., Bonni, S., and Bonni, A. (2004). Cdh1-APC controls axonal growth and patterning in the mammalian brain. Science *303*, 1026–1030.

Lauwers, E., Jacob, C., and Andre, B. (2009). K63-linked ubiquitin chains as a specific signal for protein sorting into the multivesicular body pathway. J. Cell Biol. *185*, 493–502.

Lee, S.Y., Ramirez, J., Franco, M., Lectez, B., Gonzalez, M., Barrio, R., and Mayor, U. (2014). Ube3a, the E3 ubiquitin ligase causing Angelman syndrome and linked to autism, regulates protein homeostasis through the proteasomal shuttle Rpn10. Cell Mol. Life Sci. *71*, 2747–2758.

Li, Y.R., King, O.D., Shorter, J., and Gitler, A.D. (2013). Stress granules as crucibles of ALS pathogenesis. J. Cell Biol. *201*, 361–372.

Liu, P., Gan, W., Su, S., Hauenstein, A.V., Fu, T.M., Brasher, B., Schwerdtfeger, C., Liang, A.C., Xu, M., and Wei, W. (2018). K63-linked polyubiquitin chains bind to DNA to facilitate DNA damage repair. Sci. Signal. *11*, eaar8133.

Markmiller, S., Fulzele, A., Higgins, R., Leonard, M., Yeo, G.W., and Bennett, E.J. (2019). Active protein neddylation or ubiquitylation is dispensable for stress granule dynamics. Cell Rep. *27*, 1356–1363.e3.

Markmiller, S., Soltanieh, S., Server, K.L., Mak, R., Jin, W., Fang, M.Y., Luo, E.C., Krach, F., Yang, D., Sen, A., et al. (2018). Context-dependent and disease-specific diversity in protein interactions within stress granules. Cell *172*, 590–604.e13.

Mazroui, R., Di Marco, S., Kaufman, R.J., and Gallouzi, I.E. (2007). Inhibition of the ubiquitin-proteasome system induces stress granule formation. Mol. Biol. Cell *18*, 2603–2618.

Mazroui, R., Huot, M.E., Tremblay, S., Filion, C., Labelle, Y., and Khandjian, E.W. (2002). Trapping of messenger RNA by Fragile X Mental Retardation protein into cytoplasmic granules induces translation repression. Hum. Mol. Genet. *11*, 3007–3017.

Monahan, Z., Shewmaker, F., and Pandey, U.B. (2016). Stress granules at the intersection of autophagy and ALS. Brain Res. *1649*, 189–200.

Nakayama, K., Ohashi, R., Shinoda, Y., Yamazaki, M., Abe, M., Fujikawa, A., Shigenobu, S., Futatsugi, A., Noda, M., Mikoshiba, K., et al. (2017). RNG105/caprin1, an RNA granule protein for dendritic mRNA localization, is essential for long-term memory formation. Elife *6*, e29677.

Nalavadi, V.C., Muddashetty, R.S., Gross, C., and Bassell, G.J. (2012). Dephosphorylation-induced ubiquitination and degradation of FMRP in dendrites: a role in immediate early mGluR-stimulated translation. J. Neurosci. *32*, 2582–2587.

Perez-Riverol, Y., Csordas, A., Bai, J., Bernal-Llinares, M., Hewapathirana, S., Kundu, D.J., Inuganti, A., Griss, J., Mayer, G., Eisenacher, M., et al. (2019). The PRIDE database and related tools and resources in 2019: improving support for quantification data. Nucleic Acids Res. *47*, D442–D450.

Pick, J.E., Malumbres, M., and Klann, E. (2012). The E3 ligase APC/C-Cdh1 is required for associative fear memory and long-term potentiation in the amygdala of adult mice. Learn.Mem. *20*, 11–20.

Pick, J.E., Wang, L., Mayfield, J.E., and Klann, E. (2013). Neuronal expression of the ubiquitin E3 ligase APC/C-Cdh1 during development is required for long-term potentiation, behavioral flexibility, and extinction. Neurobiol. Learn. Mem. *100*, 25–31.

Protter, D.S.W., and Parker, R. (2016). Principles and properties of stress granules. Trends Cell Biol. *26*, 668–679.

Sackton, K.L., Dimova, N., Zeng, X., Tian, W., Zhang, M., Sackton, T.B., Meaders, J., Pfaff, K.L., Sigoillot, F., Yu, H., et al. (2014). Synergistic blockade of mitotic exit by two chemical inhibitors of the APC/C. Nature *514*, 646–649.

Sharma, A., Hoeffer, C.A., Takayasu, Y., Miyawaki, T., McBride, S.M., Klann, E., and Zukin, R.S. (2010). Dysregulation of mTOR signaling in fragile X syndrome. J. Neurosci. *30*, 694–702.

Shiina, N., Yamaguchi, K., and Tokunaga, M. (2010). RNG105 deficiency impairs the dendritic localization of mRNAs for Na+/K+ ATPase subunit isoforms and leads to the degeneration of neuronal networks. J. Neurosci. *30*, 12816–12830.

Stegmuller, J., and Bonni, A. (2005). Moving past proliferation: new roles for Cdh1-APC in postmitotic neurons. Trends Neurosci. *28*, 596–601.

Sudakin, V., Ganoth, D., Dahan, A., Heller, H., Hershko, J., Luca, F.C., Ruderman, J.V., and Hershko, A. (1995). The cyclosome, a large complex containing cyclin-selective ubiquitin ligase activity, targets cyclins for destruction at the end of mitosis. Mol. Biol. Cell *6*, 185–197.

Tastet, J., Decalonne, L., Marouillat, S., Malvy, J., Thepault, R.A., Toutain, A., Paubel, A., Tabagh, R., Benedetti, H., Laumonnier, F., et al. (2015). Mutation screening of the ubiquitin ligase gene RNF135 in French patients with autism. Psychiatr. Genet. *25*, 263–267.

Tsai, N.P., Wilkerson, J.R., Guo, W., Maksimova, M.A., DeMartino, G.N., Cowan, C.W., and Huber, K.M. (2012). Multiple autism-linked genes mediate synapse elimination via proteasomal degradation of a synaptic scaffold PSD-95. Cell *151*, 1581–1594.

Vizcaino, J.A., Deutsch, E.W., Wang, R., Csordas, A., Reisinger, F., Rios, D., Dianes, J.A., Sun, Z., Farrah, T., Bandeira, N., et al. (2014). ProteomeXchange provides globally coordinated proteomics data submission and dissemination. Nat. Biotechnol. *32*, 223–226.

Wan, L., Zou, W., Gao, D., Inuzuka, H., Fukushima, H., Berg, A.H., Drapp, R., Shaik, S., Hu, D., Lester, C., et al. (2011). Cdh1 regulates osteoblast function through an APC/C-independent modulation of Smurf1. Mol. Cell *44*, 721–733.

Xie, X., Matsumoto, S., Endo, A., Fukushima, T., Kawahara, H., Saeki, Y., and Komada, M. (2018). Deubiquitylases USP5 and USP13 are recruited to and regulate heat-induced stress granules through their deubiquitylating activities. J. Cell Sci. *131*, jcs210856.

Yi, J.J., Berrios, J., Newbern, J.M., Snider, W.D., Philpot, B.D., Hahn, K.M., and Zylka, M.J. (2015). An autism-linked mutation disables phosphorylation control of UBE3A. Cell *162*, 795–807.

iScience, Volume *23*

Supplemental Information

Cdh1-APC Regulates Protein Synthesis and Stress Granules in Neurons through an FMRP-Dependent Mechanism

Arielle N. Valdez-Sinon, Austin Lai, Liang Shi, Carly L. Lancaster, Avanti Gokhale, Victor Faundez, and Gary J. Bassell

Table S1. Cdh1 interactome, Related to Figure 1

Table of proteins identified in the Cdh1 interactome following immunoaffinity chromatography and mass spectrometry analysis of FLAG-Cdh1 transfected cells. Proteins are listed from highest enrichment in the samples to lowest enrichment. N indicates nontransfected cells and C indicates FLAG-Cdh1 transfected cells. + indicates lysates co-incubated with FLAG peptide to control for nonspecific binding. Proteins that are known stress granule proteins based on Jain et al. (2016) and Markmiller et al. (2018) are indicated.

Table S2. DAVID Gene Ontology Analysis, Related to Figure 1

Proteins with at least a four-fold difference in Cdh1-transfected cells compared to control cells were entered into the DAVID Functional Annotation Bioinformatics Microarray Analysis tool (https://david.ncifcrf.gov) to classify proteins based on biological processes.

Figure S1

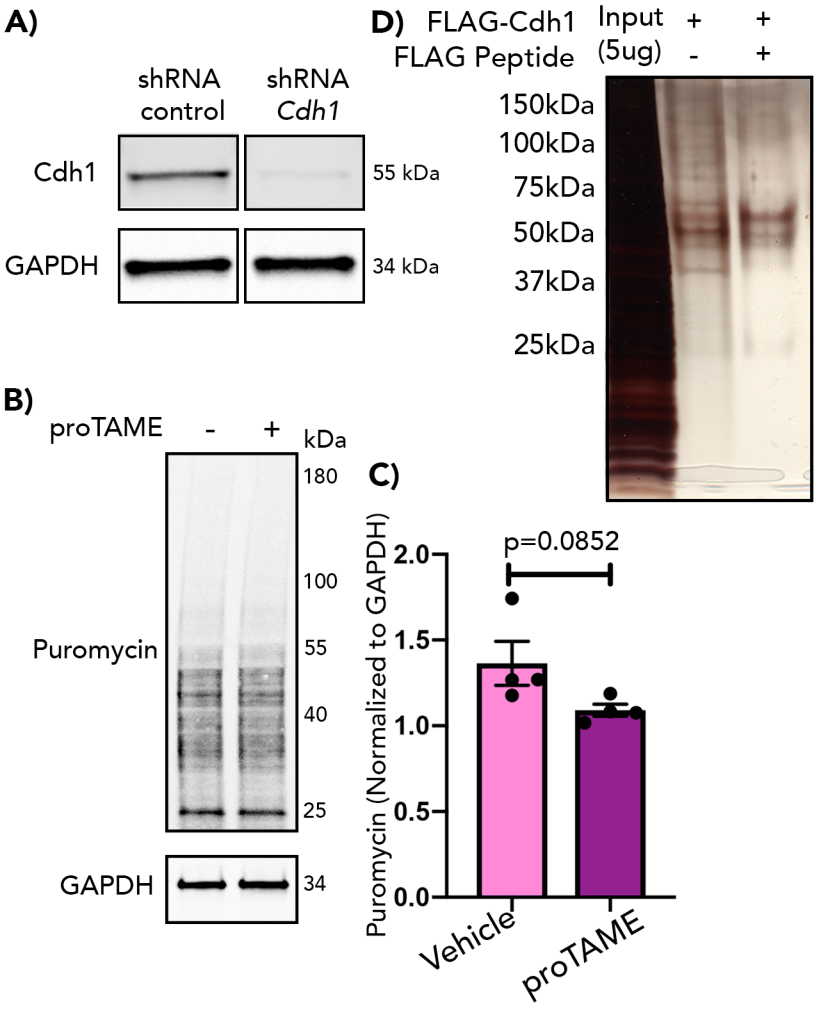
A)
shRNA control
shRNA Cdh1
Cdh1
55 kDa
GAPDH
34 kDa
B)
proTAME - +
kDa
180
100
55
40
25
Puromycin
GAPDH
34
C)
p=0.0852
Puromycin (Normalized to GAPDH)
2.0
1.5
1.0
0.5
0.0
Vehicle
proTAME
D)
FLAG-Cdh1 Input + +
FLAG Peptide (5ug) - +
150kDa
100kDa
75kDa
50kDa
37kDa
25kDa

Figure S1. Confirmation of Cdh1 knockdown and regulation of protein synthesis, Related to Figure 1

A) N2A cells were transfected with shRNA targeting *Cdh1* (*Fzr1*) or a control shRNA from Dharmacon. 72 hours after transfection, cells were lysed and immunoblotted to assess knockdown efficiency. Upon confirmation of knockdown, the Dharmacon plasmids were sent to the Emory Viral Vector core for lentiviral production. **B)** DIV 14 cortical neurons were treated with proTAME (12μM) or vehicle (DMSO) for 4 hours. 75 minutes prior to lysis, neurons underwent puromycylation (10μg/mL). **C)** Quantification of puromycin normalized to GAPDH for **B**); n=4**.** Significance calculated by Student's t test. Data are represented as mean +/- SEM. **D)** Silver stain from FLAG-Cdh1 IP in Figure 1E shows an enrichment of putative Cdh1 interacting proteins from sample without FLAG peptide co-incubation

Figure S2

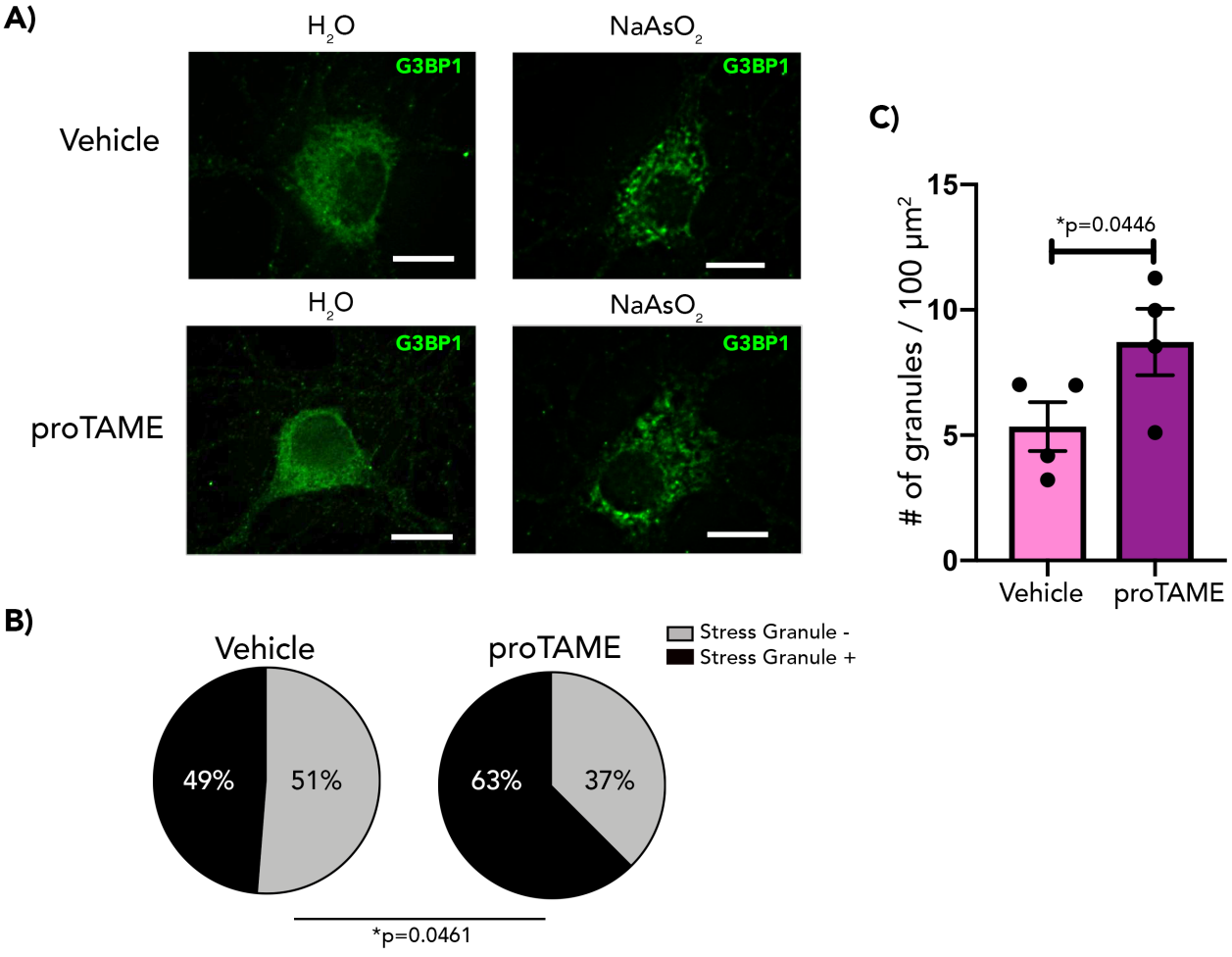
A)
H2O
NaAsO2
G3BP1
Vehicle
proTAME
B)
Vehicle
proTAME
Stress Granule -
Stress Granule +
49%
51%
63%
37%
*p=0.0461
C)
# of granules / 100 µm2
15
10
5
0
*p=0.0446
Vehicle
proTAME

Figure S2. proTAME treatment increases stress granule formation, Related to Figure 2

A) DIV 14 cortical neurons were treated with vehicle (DMSO) or proTAME for 3 hours 15 minutes. Neurons were then treated with sodium arsenite ($NaAsO_2$) (0.5mM) or water for 45 minutes hour prior to fixation. Immunofluorescence was done with antibodies against G3BP. Scale bar indicates 10μM. **B)** User-blind scoring of neurons that were stress granule positive or stress granule negative following arsenite treatment. N=60 neurons for both conditions **C)** Number of granules within the soma. Data are represented as mean +/- SEM.

Statistical significance was calculated by Z test (**B**) or by Student's t-test (**C**).

Figure S3

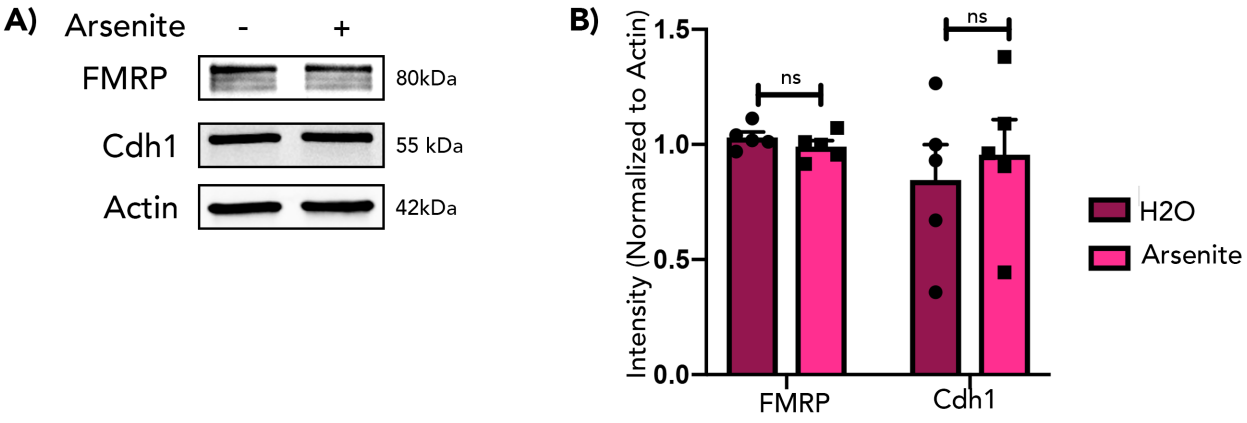
A)
Arsenite
-
+
FMRP
80kDa
Cdh1
55 kDa
Actin
42kDa
B)
Intensity (Normalized to Actin)
1.5
1.0
0.5
0.0
ns
ns
FMRP
Cdh1
H2O
Arsenite

Figure S3. **Sodium arsenite treatment does not affect FMRP or Cdh1 expression, Related to Figure 4**

A) DIV 14 cortical neurons were treated with sodium arsenite for 45 minutes and lysed and immunoblotted for FMRP, Cdh1, and actin. **B)** Quantification of FMRP and Cdh1 normalized to actin. Data are represented as mean +/- SEM. Statistical significance was calculated by two-way ANOVA.

Figure S4

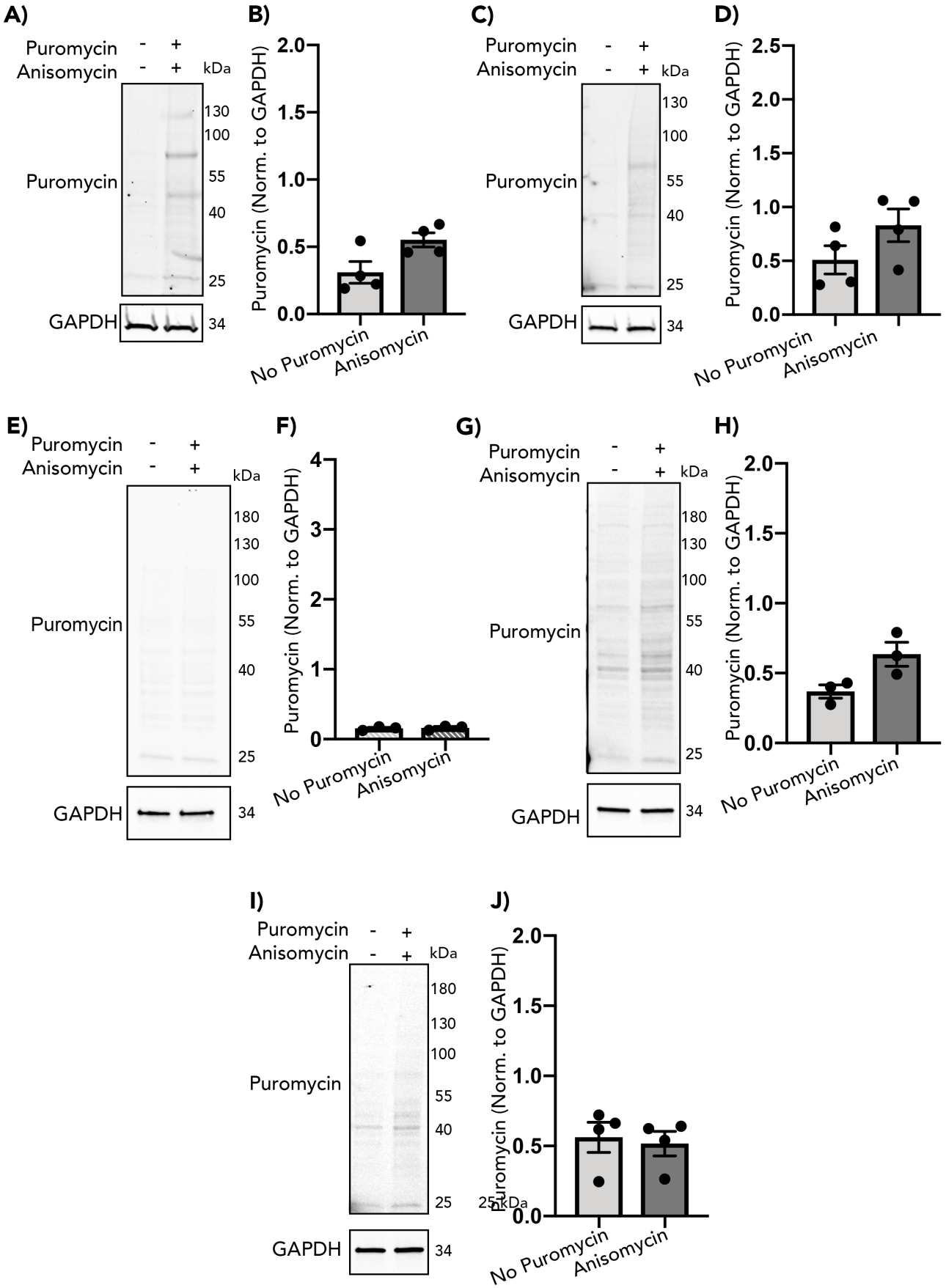
A)
Puromycin - +
Anisomycin - + kDa
130
100
Puromycin
55
40
25
GAPDH
34
B)
Puromycin (Norm. to GAPDH)
2.0
1.5
1.0
0.5
0.0
No Puromycin
Anisomycin
C)
Puromycin - +
Anisomycin - + kDa
130
100
Puromycin
55
40
25
GAPDH
34
D)
Puromycin (Norm. to GAPDH)
2.5
2.0
1.5
1.0
0.5
0.0
No Puromycin
Anisomycin
E)
Puromycin - +
Anisomycin - + kDa
180
130
100
Puromycin
55
40
25
GAPDH
34
F)
Puromycin (Norm. to GAPDH)
4
3
2
1
0
No Puromycin
Anisomycin
G)
Puromycin - +
Anisomycin - + kDa
180
130
100
Puromycin
55
40
25
GAPDH
34
H)
Puromycin (Norm. to GAPDH)
2.0
1.5
1.0
0.5
0.0
No Puromycin
Anisomycin
I)
Puromycin - +
Anisomycin - + kDa
180
130
100
Puromycin
55
40
25
GAPDH
34
J)
Puromycin (Norm. to GAPDH)
2.0
1.5
1.0
0.5
0.0
25 kDa
No Puromycin
Anisomycin

Figure S4. Controls for puromycin labeling, Related to Figures 1, 2, and S1

A,B) No puromycin and anisomycin (40μM) controls for Figure 1A. **C,D)** No puromycin and anisomycin (40μM) controls for Figure 1C. **E,F)** No puromycin and anisomycin (40μM) controls for Figure 2A. **G,H)** No puromycin and anisomycin (40μM) controls for Figure 2C. **I,J)** No puromycin and anisomycin (40μM) controls for Figure S1B.

Supplemental Information

Transparent Methods

Key Resources Table

Reagent/Resource	Source	Identifier
Antibodies		
Mouse anti-β-Actin	Thermo Fisher	AM4302
Rabbit anti-Caprin	Proteintech	15112-1-AP
Mouse anti-FLAG	Sigma	F1804
Rabbit anti-FLAG	Bethyl	A190-102A
Rabbit anti-FMR1 C terminal	Sigma	F4055
Rabbit anti-FMRP 7G-1	DSHB	7G1-1-S
Mouse anti-FMRP	BioLegend	834701
Rabbit anti-FXR1	Proteintech	13194-1-AP
Rabbit anti-GAPDH	Cell Signaling	2118S
Rabbit anti-G3BP1	Proteintech	13057-2-AP
Rabbit anti-hnRNP-U	Proteintech	14599-1-AP
Rabbit anti-HuR	Proteintech	11910-1-AP
Guinea Pig anti-MAP2	Synaptic Systems	188 004
Rabbit anti-myc	Bethyl	A190
Mouse anti-puromycin	Millipore	MABE343
Mouse anti-puromycin	Kerafast	EQ0001
Mouse anti-RPS3	Proteintech	66046-1-IG
Mouse anti-tubulin	Sigma-Aldrich	T6199
Mouse anti-Ubiquitin (FK2)	Millipore	04-263

Alexa Fluor 488 Donkey anti-Rabbit IgG (H+L)	Life Technologies	A21206
Donkey Anti-Mouse IgG Cy3	Jackson ImmunoResearch	715-165-150
Donkey Anti-Rabbit IgG Cy3	Jackson ImmunoResearch	711-165-152
Alexa Fluor 647 Goat anti-Guinea Pig IgG (H+L)	Thermo Fisher Scientific	A21450
Donkey anti-Rabbit IgG IR 800CW	LiCor	926-32213
Donkey anti-Mouse IgG IR 680LT	LiCor	926-68022
Chemicals, Peptides, and Recombinant Proteins		
Apcin	Sigma-Aldrich	SML 1503
Sodium arsenite	Millipore-Sigma	S7400
proTAME	Cayman Chemicals	25835
MG132	Sigma-Aldrich	M7449
3x FLAG Peptide	Sigma-Aldrich	F4799
Experimental Models: Cell Lines		
Neuro2A Cells	ATCC	CCL-131
Recombinant DNA		
mCherry-myc	Emory Integrated Genomics Core	n/a
mCherry-Cdh1-myc	Emory Integrated Genomics Core	n/a

Myc-DDK	Origene	PS10001
Myc-DDK-*Fzr1*	Origene	MR207910
mCMV-TurboRFP shRNA control	Dharmacon	VSC11715
mCMV-TurboRFP shRNA *Cdh1*	Dharmacon	V3SVMM08_13411185
Software and Algorithms		
Prism	GraphPad Software	Version 8
Image J	NIH	

Contact for reagent and resource sharing

Further information and requests for resources and reagents should be directed to and will be fulfilled by the corresponding author, Gary Bassell (gary.bassell@emory.edu).

Experimental model and subject details

Neuro2A Cells: Neuro2A (N2A) cells, a mouse neuroblastoma cell line, were obtained from ATCC and were cultured in DMEM media supplemented with 10% fetal bovine serum and 10 mM Hepes, (Invitrogen) at 37° C in 5% CO_2.

Primary cortical neuronal cultures: Primary cortical neurons were prepared from C57BL/6J mouse embryos (Charles River) of either sex on embryonic day 17.

Supplemental Information

For Figure 4, *Fmr1*^{HET} females (backcrossed on C57BL/6J background) were crossed with WT C57BL/6J males (Jackson Laboratory) to generate litters of pups with mixed genotypes (*Fmr1*-KO, *Fmr1*^{HET}, or wild-type). Cerebral cortices were dissected and cultured from genotyped WT and *Fmr1*-KO pups on P0-P3.

Cortices were dissociated using trypsin (Thermo Fisher Scientific) and then mechanically dissociated in Minimum Essential Medium (MEM; Fisher) supplemented with 10% Fetal Bovine Serum (Hyclone). Neurons were plated on dishes or coverslips previously coated with poly-l-lysine (Sigma) and then cultured in standard growth medium (glial conditioned neurobasal (Fisher) supplemented with glutamax (Gibco) and B27 (Invitrogen)). Culture medium was exchanged once a week until experiments were performed; cultures were maintained in an incubator regulated at 37° C in 5% CO_2. Animal protocols were approved by the institutional Animal Care and Use Committee at Emory University.

Methods Details

Transfection/Transduction

N2A cells were transfected using Lipofectamine 2000 (Invitrogen) according to manufacturer instructions 24 hours prior to experimental use.

Neurons were transduced with lentivirus at DIV 7 and were utilized at DIV 14-16 for experimental use.

Pharmacology

Supplemental Information

Apcin (2μM) (Sigma-Aldrich) or DMSO vehicle treatment was carried out for 16-18 hours. proTAME (12μM) (Cayman chemicals) or DMSO vehicle treatment was carried out for 4 hours. To induce stress granule formation, sodium arsenite (Millipore Sigma) (0.5mM) or water treatment was carried out for 45 minutes. Treatments were done at 37°C.

Puromycylation

Following transduction and/or drug treatment, neurons were washed with warm neurobasal media containing B27 and glutamax with or without 10µg/mL puromycin (Sigma-Aldrich) for 75 minutes at 37°C. The protein synthesis inhibitor anisomycin (Sigma-Aldrich) was used as a control at 40µM. Cells were then washed ice cold 1x PBS and lysed in buffer A with 0.5% Triton-X100. Lysates were sonicated and incubated on ice for 30 minutes. Lysate protein concentration was then measured by BCA assay (ThermoFisher Scientific) and then used for western blotting.

Transfected N2As were washed with warm DMEM and incubated with or without 10µg/mL puromycin (Sigma-Aldrich) for 45 minutes at 37°C. Cells were lysed and utilized for western blotting.

FLAG Immunoprecipitation

For FLAG immunoprecipitation, was performed as described by Gokhale et al. (Gokhale et al., 2012). N2A cells were transfected with FLAG-Cdh1 (Origene MR207910) with PolyMag Neo (OZ Biosciences) for 24 hours, as per manufacturer instructions. Cells were rinsed twice with 1x PBS and lysed in buffer A (150 mM NaCl, 10mM HEPES, 1mM EGTA, and 0.1mM $MgCl_2$, pH 7.4) with 0.5% Triton-X100 and Complete anti-protease (Roche). Cells were sonicated followed by incubation on ice for 30 minutes. Cell lysates were centrifuged at 16,100 x g for 15 minutes.

Clarified supernatant was collected and protein concentration was measured by Bradford Assay (Bio-Rad). 500ug of protein extract was added to 30uL of Dynabeads (Invitrogen 11031) and incubated for 3 hours at 4° C. In some assays, immunoprecipitation was performed in the presence of antigenic 3x-FLAG peptide (340uM, Sigma F4799) as a control. After incubation, beads were washed 6 times with buffer A with 0.1% Triton X-100. Proteins were eluted from the beads with 2-hour incubation on ice with buffer A and 340uM 3x-FLAG-antigenic peptide. Samples were resolved by SDS-PAGE and contents analyzed by immunoblot or silver stain. For proteomic analysis, proteins eluted from the beads were combined and concentrated by TCA precipitation.

Endogenous Cdh1 Immunoprecipitation

Embryonic brain tissues were collected from E17 (C57BL/6) mouse embryos. Brain tissues were lysed in buffer A (150mM NaCl, 10mM HEPES, 1mM EGTA, and 0.1mM MgCl2, pH 7.4) with 0.5% TX-100 and Halt Protease and Phosphatase inhibitor (Thermo Fisher 78441) by sonication. After incubation on ice for 30 minutes, tissue lysates were centrifuged at 12,000 x g for 30 minutes. Clarified supernatants were collected and protein concentrations were measured by BCA assay (Thermo Fisher 23227). Protein lysates were diluted to 5ug/ul by lyse buffer and 100ul of protein lysates were mixed with 400ul of buffer A as immunoprecipitation input. 20uL of ProteinG Dynabeads (Thermo Fisher 10-003-D) were washed by buffer A and then incubated with either 2ug rabbit anti-FZR1 (Cdh1) (Proteintech 16368-1) antibody or 2ug normal rabbit IgG (Millipore 12-370) for 2 hours. After incubation, beads were washed by buffer A, and then incubated with immunoprecipitation input at 4C overnight. After incubation, beads were washed sequentially by buffer A with 0.1% Triton X-100, buffer A with 50mM NaCl and 0.25% Triton X-100, and buffer A with 100mM NaCl and 0.5% Triton X-100. Proteins were eluted from the beads with 50ul of

0.2mM glycine, pH2.6. Samples were run on a 4-20% Criterion TGX gel (Bio-Rad 4561093) and transferred onto Nitrocellular membrane. Blots were blocked with 5% milk in 1x PBST for 1hr at room temperature, and then incubated overnight at 4C with primary antibody diluted in blocking buffer. Blots were incubated with HRP conjugated secondary antibodies (ABclonal AS014 and AS003) diluted in blocking buffer for 1hr at room temperature. Three 10-minute washes with PBST were performed before and after addition of secondary antibodies. Blots were developed using Tanon High-sig ECL kit (ABclonal 180-501) and Amersham Hyperfilm (GE Lifesciences).

Western Blotting

For FLAG immunoprecipitation experiments, samples were run on a 4-20% Criterion TGX gel (Bio-Rad) and transferred onto PVDF membrane. Blots were blocked with 5% milk in 1x TBS-0.5%. TritonX-100 for 30 minutes at room temperature. Blots were incubated overnight at 4°C in primary antibody diluted in 3% BSA, 0.5% Sodium Azide, and 1x PBS. Blots were incubated in HRP secondary antibodies (Sigma) diluted in 5% milk in 1x TBS-0.5% TritonX-100 for 40 minutes at room temperature. Three 5-minute washes with TBS-0.5% TritonX-100 were performed before and after addition of secondary antibodies. Blots were developed using Western Lightning ECL Pro (Perkin Elmer) and Amersham Hyperfilm (GE Lifesciences).

For puromycin labeling experiments, 20µg of protein per sample were resolved by SDS-PAGE on a 4-20% Mini-Protean TGX protein gel (Bio-Rad) and transferred to a nitrocellulose membrane. Blots were blocked in Odyssey Blocking Buffer (LI-COR), and incubated overnight at 4°C in primary antibodies diluted in a 1:1 mix of blocking buffer and PBS-Tween-0.1%. Blots were incubated in secondary antibodies (LI-COR) diluted in PBS-Tween-0.1% for 1 hour at room

temperature. Three 10-minute washes with PBS-Tween-0.1% were performed before and after addition of secondary antibodies. Blots were viewed on a Bio-Rad ChemiDoc MP. Protein levels were assessed by quantitative densitometry using ImageJ.

Proteomics Analysis

Samples were analyzed for interactome analysis by MS Bioworks (http://www.MSBioworks.com). Proteomics samples were separated on a 10% Bis-Tris Novex mini-gel (Invitrogen) using the MES buffer system. The gel was stained with coomassie and excised into ten equally sized segments. Gel segments were processed using a robot (Progest, DigiLab). First, gel segments were washed with 25mM ammonium bicarbonate followed by acetonitrile. They were then reduced with 10mM dithiothreitol at 60°C followed by alkylation with 50mM iodoacetamide at RT. Then, segments were digested with trypsin (Promega) at 37°C for 4 hours. They were then quenched with formic acid and the supernatant was analyzed directly without further processing. The gel digests were analyzed by nano LC/MS/MS with a Waters NanoAcquity HPLC system interfaced to a ThermoFisher Q Exactive. Peptides were loaded on a trapping column and eluted over a 75µm analytical column at 350nL/min; both columns were packed with Luna C18 resin (Phenomenex). The mass spectrometer was operated in data-dependent mode, with MS and MS/MS performed in the Orbitrap at 70,000 FWHM resolution and 17,500 FWHM resolution, respectively. The fifteen most abundant ions were selected for MS/MS. Data were searched using a local copy of Mascot.

Bioinformatic Analysis

Supplemental Information

Gene ontology analysis was performed with Database Annotation, Visualization and Integrated Disovery (DAVID, https://david.ncifcrf.gov). Cytoscape with Enrichment Map plugin for visualizing DAVID outputs was used to represent the Biological Processes enriched within the Cdh1 interactome.

Immunofluorescence:

Cells were fixed in 4% paraformaldehyde for 15 minutes, washed three times for 10 minutes in PBS. Cells were blocked for 1 hour in blocking solution consisting of 5% normal donkey serum, 0.1% bovine serum albumin, and 0.1% Triton-X 100 in PBS. Cells were incubated overnight in primary antibodies diluted in blocking solution. The next day, cells were washed 3 times for 10 minutes in PBS. They were incubated in secondary antibodies in blocking solution for one hour at room temperature. Cells were washed 3 times for 10 minutes. Coverslips with the cells were dipped in ultrapure water and then mounted using Prolong Gold Antifade mounting media (Invitrogen). Cells were imaged using a Keyence BZ-X810 or a Nikon Eclipse TE300 widefield fluorescence microscope with a 60X objective. Z-series were acquired at 0.2μm steps and image stacks were deconvolved using AutoQuant X3 software and a 3-D blind algorithm.

Quantification and statistical analysis

Statistical analyses and graphs were prepared in GraphPad Prism (v.8). All data are expressed as mean +/- SEM. Replicates are reported in the figure legends or directly on the figures. For all experiments, α was set as 0.05. See figure legends for specific statistical analyses.

Quantification of Stress Granules

Supplemental Information

Coverslips for immunocytochemistry were blinded during imaging and quantification. Imaged neurons were classified as being stress granule positive or negative based on G3BP1 staining. Diffuse G3BP1 staining was classified as stress granule negative whereas cells with punctate G3BP1 staining were classified as stress granule positive. The total number of stress granule positive or negative neurons for each condition were then input into GrapPad Prism and a z-test was ran on the data.

Number of stress granules in the soma of each cell were quantified using Image J plugin TrackMate (Tinevez et al., 2017) with the Laplacian of Gaussian detector (threshold set from 5-15). Total area of the cell body was quantified using Image J plugin Mitomorphology macro (Dagda et al., 2009) with threshold set as 130-180. The number of granules were normalized to the cell body area.

Supplemental References

Dagda, R.K., Cherra, S.J., 3rd, Kulich, S.M., Tandon, A., Park, D., and Chu, C.T. (2009). Loss of PINK1 function promotes mitophagy through effects on oxidative stress and mitochondrial fission. J Biol Chem *284*, 13843-13855.

Gokhale, A., Larimore, J., Werner, E., So, L., Moreno-De-Luca, A., Lese-Martin, C., Lupashin, V.V., Smith, Y., and Faundez, V. (2012). Quantitative proteomic and genetic analyses of the schizophrenia susceptibility factor dysbindin identify novel roles of the biogenesis of lysosome-related organelles complex 1. J Neurosci *32*, 3697-3711.

Tinevez, J.Y., Perry, N., Schindelin, J., Hoopes, G.M., Reynolds, G.D., Laplantine, E., Bednarek, S.Y., Shorte, S.L., and Eliceiri, K.W. (2017). TrackMate: An open and extensible platform for single-particle tracking. Methods *115*, 80-90.